JGR Atmospheres

RESEARCH ARTICLE
10.1029/2024JD041482

Special Collection:
Emerging air pollution: emissions, chemistry, and health and climate effects

Impact of Heatwaves and Declining NO_x on Nocturnal Monoterpene Oxidation in the Urban Southeastern United States

N. S. Desai[1], A. C. Moore[2], A. P. Mouat[2], Y. Liang[3,4], T. Xu[3], M. Takeuchi[2,5], H. O. T. Pye[6], B. Murphy[6], J. Bash[6], I. B. Pollack[7], J. Peischl[8,9], N. L. Ng[1,2,3], and J. Kaiser[1,2]

[1]School of Earth and Atmospheric Sciences, Georgia Institute of Technology, Atlanta, GA, USA, [2]School of Civil and Environmental Engineering, Georgia Institute of Technology, Atlanta, GA, USA, [3]School of Chemical and Biomolecular Engineering, Georgia Institute of Technology, Atlanta, GA, USA, [4]Now at Thrust of Sustainable Energy and Environment, The Hong Kong University of Science and Technology (Guangzhou), Guangdong, China, [5]Now at Department of Mechanical Engineering, University of Colorado at Boulder, Boulder, CO, USA, [6]Office of Research and Development, USA Environmental Protection Agency, Research Triangle Park, NC, USA, [7]Department of Atmospheric Science, Colorado State University, Fort Collins, CO, USA, [8]Cooperative Institute for Research in Environmental Sciences, University of Colorado Boulder, Boulder, CO, USA, [9]NOAA Chemical Sciences Laboratory, Boulder, CO, USA

Key Points:

- Nitrate radical (NO_3) continues to control nocturnal boundary layer monoterpene oxidation in the urban SE US
- Regional model overpredicts oxidant concentrations and fractional NO_3 contribution to monoterpene loss
- Extreme heat events increase nighttime NO_3 concentrations, monoterpene oxidation rates, and gas-phase organic nitrate production

Supporting Information:

Supporting Information may be found in the online version of this article.

Correspondence to:

J. Kaiser,
jennifer.kaiser@ce.gatech.edu

Citation:

Desai, N. S., Moore, A. C., Mouat, A. P., Liang, Y., Xu, T., Takeuchi, M., et al. (2024). Impact of heatwaves and declining NO_x on nocturnal monoterpene oxidation in the urban southeastern United States. *Journal of Geophysical Research: Atmospheres*, *129*, e2024JD041482. https://doi.org/10.1029/2024JD041482

Received 14 JUN 2024
Accepted 17 AUG 2024

Abstract Nighttime oxidation of monoterpenes (MT) via the nitrate radical (NO_3) and ozone (O_3) contributes to the formation of secondary organic aerosol (SOA). This study uses observations in Atlanta, Georgia from 2011 to 2022 to quantify trends in nighttime production of NO_3 (PNO_3) and O_3 concentrations and compare to model outputs from the EPA's Air QUAlity TimE Series Project (EQUATES). We present urban-suburban gradients in nighttime NO_3 and O_3 concentrations and quantify their fractional importance (F) for MT oxidation. Both observations and EQUATES show a decline in PNO_3, with modeled PNO_3 declining faster than observations. Despite decreasing PNO_3, we find that NO_3 continues to dominate nocturnal boundary layer (NBL) MT oxidation ($F_{NO3} = 60\%$) in 2017, 2021, and 2022, which is consistent with EQUATES ($F_{NO3} = 80\%$) from 2013 to 2019. This contrasts an anticipated decline in F_{NO3} based on prior observations in the nighttime residual layer, where O_3 is the dominant oxidant. Using two case studies of heatwaves in summer 2022, we show that extreme heat events can increase NO_3 concentrations and F_{NO3}, leading to short MT lifetimes (<1 hr) and high gas-phase organic nitrate production. Regardless of the presence of heatwaves, our findings suggest sustained organic nitrate aerosol formation in the urban SE US under declining NO_x emissions, and highlight the need for improved representation of extreme heat events in chemistry-transport models and additional observations along urban to rural gradients.

Plain Language Summary Monoterpenes are important precursors of secondary organic aerosol (SOA), which influence air quality and climate. At night, they react with the nitrate radical (NO_3) and ozone (O_3). Trends in these two oxidants and their role on air quality in the southeastern United Sates (SE US) is partially dictated by changes in nitrogen oxide ($NO_x = NO + NO_2$) emissions which have declined in recent years. We find that NO_3 dominates present-day monoterpene loss in the summer, and may continue to do so even as NO_x concentrations decrease in the future. We show that heatwaves in the SE US further elevate both O_3 and NO_3 concentrations at night, with a larger relative importance for NO_3. We compare observations to a regional air quality model, and find the model overpredicts both oxidant concentrations. This overprediction may impact model-based studies of future nighttime chemistry.

1. Introduction

Oxidation of volatile organic compounds (VOCs) contributes to the formation of secondary organic aerosol (SOA), pollutants that degrade air quality. The primary oxidants at night are the nitrate radical (NO_3) and ozone (O_3), which are both highly reactive with monoterpenes (MT, $C_{10}H_{16}$). Observations show that MT are the primary contributor to SOA in the southeastern US (SE US) (Xu et al., 2018; Zhang et al., 2018). Because organic nitrate aerosol formed from MT + NO_3 reactions comprises up to 70% of the SOA budget in the SE US (Bates et al., 2022; Fry et al., 2009; Xu, Suresh, et al., 2015), MT-SOA and total SOA may decline with lower NO_3 concentrations (Xu, Guo, et al., 2015). Under lower NO_3, the MT + O_3 reaction increases in relative importance. Depending on the assumed yield of this reaction and trends in total atmospheric oxidation capacity, MT-SOA may

either decrease with decreasing NO_x emissions (Pye et al., 2019; Xu, Guo, et al., 2015), or be buffered against declines in nitrate-induced oxidation by higher-yield MT + O_3 reactions (Liu et al., 2023). A critical need for understanding trends in SOA and its composition in the SE US is quantifying trends in nighttime oxidant levels and their relative importance for MT oxidation. Here, we examine the gas-phase chemistry and meteorological parameters that determine trends in NO_3, O_3, and MT concentrations and resultant MT lifetimes at two locations in the urban SE US.

NO_3 is formed from the reaction between nitrogen dioxide (NO_2) and O_3 (Equation 1). NO_3 radical production ($PNO_3 = k_1[NO_2][O_3]$) is a nonlinear function of NO_x ($NO_x = NO + NO_2$) emissions (Wang, Wang, et al., 2023; Wang, Xi, et al., 2023). In NO_x-limited regions, decreasing NO_x emissions decreases total odd oxygen ($O_x = NO_2 + O_3$) and resultant PNO_3 (Haslett et al., 2023). The opposite is the case in highly polluted urban environments, where the NO + O_3 titration reaction (Equation 2) decreases PNO_3. In these regions, decreasing NO_x emissions can increase PNO_3.

$$NO_2 + O_3 \rightarrow NO_3 + O_2 \quad (1)$$

$$NO + O_3 \rightarrow NO_2 + O_2 \quad (2)$$

$$NO + NO_3 \rightarrow 2\,NO_2 \quad (3)$$

$$VOC + NO_3 \rightarrow \text{Products} \quad (4)$$

While PNO_3 is often used as a proxy for the importance of NO_3 oxidation, NO_3 radical concentrations depend on both production and loss. On the global scale, biogenic VOCs (BVOCs) are the dominant NO_3 sink (Equation 4) (Brown & Stutz, 2012; Fry et al., 2014). In urban environments, anthropogenic VOCs (AVOCs) and NO (Equation 3) regulate the trends and magnitude of NO_3 concentrations (Brown et al., 2011; Stutz et al., 2010).

Regional trends in PNO_3 and NO_3 abundance have been examined in a number of observational and model-based studies. These studies provide differing perspectives based on the location of the observations, resolution of the models, and their associated emission inventories. Edwards et al. (2017) provide a regionally averaged perspective using aircraft observations in the residual layer during the 2013 Southeast Nexus (SENEX) campaign. They find a slightly higher NO_3 importance relative to O_3 for total BVOC loss (53% and 47%, respectively), and conclude that 2013 marked a transition year toward an O_3-dominated future. In contrast, Wang, Wang, et al. (2023) found only a small, statistically insignificant decrease in PNO_3 across the majority of ground-based long-term measurement locations in the US from 2014 to 2019. Vertical gradients in VOCs, O_3 and NO_3 can cause significant differences in PNO_3 and oxidation rates compared to at the surface (Brown et al., 2007, 2013; Stutz et al., 2004). Using the CAM6 model (horizontal resolution = 0.95° × 1.25°), Liu et al. (2023) find large decreases in both surface NO_3 and O_3 concentrations across the Eastern US from 1988 to 2019, which is consistent with other modeling studies (Li et al., 2018). Many ground sites are located in or near urban areas, and models may represent a more regionally averaged trend depending on spatial resolution and their emission inventories.

The short lifetime of NO_3 leads to significant spatial heterogeneity in its abundance and relative importance. For example, a study focused on the Yangtze River Delta, China finds similar PNO_3 across the region, but much larger NO_3 abundance in the urban core due to a larger biogenic VOC + NO_3 sink in the suburban regions (Chen et al., 2019). Similar patterns may be expected in the urban SE US, where biogenic and anthropogenic emissions are both high, but somewhat spatially segregated (Yu et al., 2016). Examining multiple locations across a city allows us to understand the representativeness of long-term measurements at a given site, and aids in the interpretation of trends and discussion of model/observation differences.

An increasingly important consideration for trends in MT oxidation and related SOA formation is the impact of climate-related changes in summertime temperature, biogenic emissions, and nighttime pollution events. Extreme heat events, characterized by periods of maximum temperatures above 32°C for at least 2 consecutive days, are becoming more intense and prevalent under a warming climate (Fischer et al., 2013; Vose et al., 2017). The SE US is projected to experience an increase of 40–50 days exceeding 32°C by 2035–2065 (Vose et al., 2017). High daytime temperatures increase both biogenic emissions and O_3 production. This may counteract the decline in total oxidant concentrations expected with decreased NO_x emissions on the regional scale. Additional

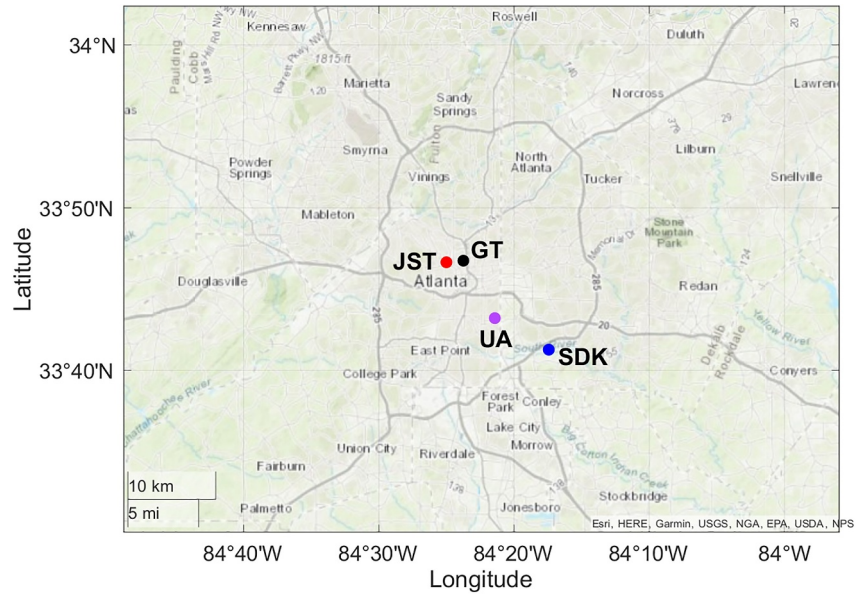

Figure 1. Map of Atlanta, GA with the Jefferson Street (JST, red), Georgia Tech (GT, black), United Avenue (UA, purple), and SDK PAMS (SDK, blue) field sites (Esri).

observational studies are needed to help understand the complex roles of meteorological conditions on nocturnal oxidant concentrations and their impact on MT oxidation amid future reductions in NO_x.

This study quantifies the trend and spatial pattern of nighttime summer PNO_3 in the urban SE US using NO, NO_2, and O_3 measurements from two field sites in the Atlanta metropolitan area spanning from 2011 to 2022. Additional VOC observations in 2017, 2021, and 2022 allow us to quantify NO_3 and the relative importance of NO_3 and O_3 for MT oxidation at these two locations. We compare our results to the regional analysis by Edwards et al. (2017) in the same year and discuss differences in regimes inferred from observations at different altitudes. We also compare observationally based PNO_3 and relative oxidant importance to model outputs from the EQUATES, the EPA's Air QUAlity TimE Series Project for 2011–2019 (Foley et al., 2023). We discuss the differences between a model- and observation-based analysis and identify the improvements needed in models to better capture the future of MT oxidation in the SE US. We present two case studies to demonstrate the impact of extreme heat events on MT oxidation. Finally, we briefly discuss the implications of nighttime oxidant budgets for future MT-SOA formation in the SE US.

2. Methods

2.1. Observations in Atlanta

We use summertime (June–August) observations taken at two locations in Atlanta, GA, located approximately 15 km a part, as shown in Figure 1. These sites represent an urban core (JST/GT), and an urban background (SDK) environment. The JST/GT sites are heavily influenced by urban traffic, while SDK is more forested with surrounding residential properties. Wind roses for each location are provided in the Supporting Information S1 (Figure S4 and S5). Unless otherwise stated, all values are calculated from hourly averaged data sets. Observations are explored from 21 to 06 local time (LT) each night.

The South DeKalb (SDK) site (33.6878°N, 84.2905°W, 308 m elevation) is a Photochemical Assessment Monitoring Site (PAMS) location operated by the Georgia Environmental Protection Division (EPD). We use temperature, pressure, O_3, NO, NO_2 from 2011 to 2022. Interferences associated with chemiluminescence-based NO_2 measurements (Reed et al., 2016) are discussed in the Supporting Information S1, and have minimal impact on our analysis. We include VOCs (measured via gas chromatography) in our analysis beginning in 2021, when α- and β-pinene observations became available. Considering only these species, α-pinene was the dominant MT in 2021 (71%) and 2022 (83%). Ozone observations from the United Ave (UA). site, also operated by the EPD, are

used to support our analysis. Observations for UA and SDK sites were accessed using the EPA AQS API (Air Quality System Application Programming Interface) (https://aqs.epa.gov/aqsweb/documents/data_api.html).

The Jefferson Street (JST) site (33.7775°N, 84.4167°W, 300 m elevation) was part of the SouthEastern Aerosol Research and Characterization (SEARCH) network. A detailed site description, measurement approaches, and uncertainties are available in prior literature (Blanchard & Hidy, 2018; Hansen et al., 2003, 2006; Xu, Suresh, et al., 2015). We use measurements of O_3, NO, NO_2, temperature and pressure from 2011 to 2018. Speciated MT (α- and β-pinene, limonene) and other VOC measurements taken via gas chromatography are available in 2017. Median nighttime MT speciation is 42% α-pinene, 48% β-pinene, and 10% limonene.

While the SEARCH network discontinued in 2017, measurements taken at Georgia Tech's campus, located approximately 1.5 km east of JST, in more recent years provides an extension of the urban-core data set (Xu, Suresh, et al., 2015). Measurements were taken on the rooftop of the Ford Environmental Science and Technology building (33.7791°N, 84.3958°W, 315 m elevation) in August–September 2022. NO was measured using the Thermo Fisher Scientific Model 42i analyzer, with an instrument precision of 0.4 ppbv. Unfortunately, NO_2 measurements are not available for this period due to calibration errors. These calibration errors did not impact NO measurements. O_3 was measured using a Thermo Fisher Scientific Model 49C UV photometric analyzer, with an instrument precision of 1 ppbv. Meteorological parameters were recorded at Georgia Tech's Bobby Dodd Stadium, located 800 m south of the measurement site.

In August–September 2022, MT measurements at Georgia Tech were made using an Ionic on Proton Transfer Reaction Time of Flight Mass Spectrometer (PTR-ToF-MS) 4000. Experimental setup and calibration of the PTR-ToF-MS follows the methods of Peng et al. (2022), and are described further in the Supporting Information S1 (Text S2). We calibrate the MT signal (m/z 137) using a gas standard (MESA) containing α-pinene. PTR MT observations are used only for a relative comparison of concentrations on heatwave and non-heatwave nights.

Gas- and particle-phase oxygenated VOCs (OVOCs), were measured using the Filter Inlet for Gases and Aerosols High Resolution Time-of-Flight Chemical Ionization Mass Spectrometer (FIGAERO-CIMS) using iodide (I^-) as the reagent ion. Experimental setup of the FIGAERO-CIMS is described in prior literature (Chen et al., 2020; Takeuchi & Ng, 2019). We use observations of $C_{10}H_{17}NO_5$ (amu 358.02), a precursor of organic nitrate aerosol (Ayres et al., 2015; Boyd et al., 2015; Lambe et al., 2023; Nah et al., 2016; Takeuchi & Ng, 2019) and $C_{10}H_{16}O_8$ (amu 391), a highly oxygenated molecule (HOM, $>O_{5-6}$) (Bianchi et al., 2019) produced from MT ozonolysis. We sum the gas-phase signal and gas-equivalent signal of the particle-phase for both species, to account for differences in gas-particle partitioning behavior and volatilities of the compounds. Species are reported in normalized counts per second (ncps), as analyte-specific calibrations were not available. Given the proximity of JST and GT, we combine these measurements to create one data set spanning 2011–2022 representing the urban core. For simplicity, the combined JST/GT data set is referred to as "JST" throughout our analysis.

2.2. SENEX Observations

Observations taken aboard the NOAA WP-3D aircraft during SENEX in 2013 are provided by the NOAA Chemical Sciences Laboratory (Warneke et al., 2016). We use NO, NO_2, O_3, temperature and pressure from two of the three night flights during the campaign, 19 June and 02 July 2013, analogous to Edwards et al. (2017). Only observations sampled below 1 km are included in the analysis to capture residual layer chemistry. Information regarding measurement techniques and uncertainties can be found in prior literature (Pollack et al., 2010; Ryerson et al., 1999, 2000; Warneke et al., 2016).

2.3. EQUATES

The Environmental Protection Agency's (EPA) Air QUality TimeE Series (EQUATES) Project provides Community Multiscale Air Quality (CMAQ) v5.3.2 model outputs from 2002 to 2019 over the contiguous US at a 12×12 km^2 horizontal resolution (Foley et al., 2023; https://doi.org/10.5281/zenodo.4081737). We use hourly averaged temperature, surface pressure and concentrations of NO, NO_2, O_3, NO_3, α-pinene (APIN), and other terpenes (TERP) from the first (surface layer) of the model for the grid cells containing JST and SDK June–August 2011–2019. The EQUATES base year emissions are from the 2017 National Emissions Inventory (NEI), which are then used to estimate emissions for the entire 2011–2019 time period. EQUATES also uses year-specific information when possible, such as for monitored electric generating units, wildland fires, and biogenic

vegetation sources (Bash et al., 2016). EQUATES includes the impact of AVOCs as described in the CB6r3 chemistry (Luecken et al., 2019). The CMAQ version here has been extensively evaluated against AQS observations over the U.S (Appel et al., 2021; Benish et al., 2022). Trends in NO_x emissions from the 2017 NEI have been shown to have good agreement with trends in surface NO_2 concentrations from the AQS and SEARCH networks between 2005 and 2017 (Silvern et al., 2019).

2.4. Calculation of PNO_3, NO_3, and MT Loss Rates

For calculation of observed PNO_3 and all other reaction rates, we use rate coefficients from the Master Chemical Mechanism (MCM) v3.3.1 (Bloss et al., 2005; Jenkin et al., 1997, 2003, 2015; Saunders et al., 2003). For calculating modeled reaction rates, we use the rate constants associated with CMAQ's lumped mechanism. Temperatures and pressures used correspond to the measured or modeled mixing ratios.

We calculate steady-state $[NO_3]$ for the time periods when both NO_2 and VOC measurements are available (2017 JST, 2021–2022 SDK) using Equation 5:

$$[NO_3]_{ss} \approx \frac{PNO_3}{\sum_i k_{NO_3+VOC_i}[VOC]_i + k_{NO_3+NO}[NO]} \quad (5)$$

We include loss terms for all measured VOCs, though we find AVOCs contributed <1% to NO_3 loss at both sites. A complete list of VOCs included can be found in the Supporting Information S1.

We find the NO_3 + NO reaction (Equation 3) at night contributes significantly to NO_3 loss at JST (median of 87%) and negligible contribution at SDK (median 0% across 2021–2022).

The temperature-dependent reversible reaction of NO_2 and NO_3 to produce N_2O_5 followed by the heterogenous reaction of N_2O_5 to HNO_3 is a permanent NO_3 sink (Brown et al., 2006, 2011; Ravishankara, 1997). However, the rapid NO_3 loss rate ($\tau \sim$ seconds) combined with warm temperatures during summer nights in Atlanta favors NO_3 in its equilibrium with N_2O_5 (K_{eq}). Using an uptake coefficient of $\gamma_{N_2O_5} = 0.01$ and aerosol surface area density A of 300 μm^2 cm^{-3}, the loss rate constant was found to be $k_{N2O5} = 0.25\,\bar{\nu}\,A\,\gamma_{N_2O_5} \sim 10^{-4}$ s^{-1} for the reaction $N_2O_5 \rightarrow 2\,HNO_3$ (Riemer et al., 2003). The uptake coefficient is an upper bound due to the high organic fraction (>60%) of aerosol measured at JST during operation of the SEARCH network (Kim et al., 2015; Rattanavaraha et al., 2017; Xu, Suresh, et al., 2015). The aerosol surface area density is representative of previous ground measurement and modeling studies in the southern and eastern US (Bergin et al., 2022). Combining this with the equilibrium constant for the NO_2 to NO_3 conversion, we find $(K_{eq}[NO_2])^{-1}k_{N2O5} \sim 10^{11}$ s^{-1}, which is <1% of the total NO_3 loss rate and therefore negligible for our analysis.

The fraction of nighttime speciated MT oxidation attributed to NO_3 (F_{NO3}) (Equation 6) is calculated for both observational and modeled data sets. Measured α-pinene and β-pinene are included for calculations at both sites, along with limonene at JST. Although ozonolysis and NO_3 oxidation can both form the hydroxyl radical (OH) at night, its contribution to MT loss and SOA formation is usually small (Zhang et al., 2018). However, in nighttime environments where MT + O_3 reactions are prominent, modeled nighttime OH concentrations and their contribution to VOC loss can be high (Ren et al., 2003). We find that median nocturnal F_{OH} in EQUATES in 2019 is 11% and 8% at JST and SDK, respectively. In the CB6r3 mechanism used in EQUATES, MT + O_3 yields OH. Additionally, nighttime isoprene concentrations in EQUATES are underestimated at both locations (Figure S6 in Supporting Information S1). So, OH concentrations are likely overestimated in the model. Because we have no observational constraints for OH, we omit the contribution of OH-initiated oxidation in our analysis. As a result, calculated MT lifetimes and fractional oxidant importance therefore represent an upper bound.

Relative oxidant importance and total reactivity varies for each monoterpene isomer. For example, the observed median nighttime reactivity (and F_{NO3}) of β-pinene and limonene in 2017 are 1.27×10^{-5} s^{-1} (57%) and 9.65×10^{-5} s^{-1} (37%), respectively. In an environment where β-pinene was the most abundant monoterpene measured (such as JST), F_{NO3} may be higher than if limonene dominated. This shows that site-to-site variability in MT composition can impact F_{NO3}. Speciated MT measurements are best suited for understanding F_{NO3} and organic nitrate production.

$$F_{NO3} = \frac{\sum_i k_{NO_3+MT_i}[NO_3]_{ss}[MT_i]}{\sum_i k_{O_3+MT_i}[O_3][MT_i] + \sum_i k_{NO_3+MT_i}[NO_3]_{ss}[MT_i]} \quad (6)$$

3. Results and Discussion

3.1. Trends and Drivers of Nocturnal Boundary Layer PNO_3

Figure 2 shows the observed and modeled trends in NO_2, O_3, and PNO_3 at JST and SDK. Observations of NO_2 and O_3 are higher at JST than SDK, leading to higher calculated PNO_3 in the urban core. At both sites, NO_2 shows a statistically significant ($p < 0.05$) decline from 2011 to 2022 (-0.70 ± 0.15 ppbv y^{-1} at JST and -0.55 ± 0.19 ppbv y^{-1} at SDK), while O_3 concentrations remain flat. Trends were tested and calculated using ordinary least squares linear regression. Observed PNO_3 is impacted by large relative night-to-night variability in O_3—attributed to titration. As a result, there is a weak, statistically significant ($p < 0.05$) trend in observed PNO_3 (-0.049 ppbv hr^{-1} y^{-1} at JST and -0.014 ppbv hr^{-1} y^{-1} at SDK). This weak trend in PNO_3 calculated from observations was also seen at other ground-sites across the US (Wang, Wang, et al., 2023).

EQUATES also shows higher NO_2 and PNO_3 at JST relative to SDK. Both the magnitude and trend in NO_2 are similar to observations (-0.64 ± 0.12 ppbv y^{-1} at JST and -0.83 ± 0.10 ppbv y^{-1} at SDK). EQUATES shows constant nighttime O_3 at both sites, but overestimates O_3 concentrations by 30% and 70% at JST and SDK, respectively. Whereas observed PNO_3 is impacted by O_3 variability, modeled O_3 is much more consistent, and therefore modeled PNO_3 more closely reflects the trends in NO_2. The model displays a similar continual reduction in PNO_3 (-0.057 ppbv hr^{-1} y^{-1} at JST and -0.066 ppbv hr^{-1} y^{-1} at SDK). The high biases in O_3 lead to an overprediction of PNO_3 in EQUATES.

Models commonly overestimate nighttime O_3 by > 10 ppbv, particularly in the SE US (Appel et al., 2021; Fiore et al., 2009; Makar et al., 2017). One explanation for the large differences in observed and measured O_3 is the model's inability to capture O_3 titration. In the observational data set, 80% of all nights at SDK and 51% at JST in 2017 had exceptionally low O_3 (0–5 ppbv) and high NO (>1 ppbv). In EQUATES, there are very few low O_3/high NO nights at either location (3% and 10% at SDK and JST, respectively). Additionally, on >80% low O_3 nights at SDK in 2017, O_3 was also low at two other ground sites across Atlanta: JST and United Avenue (10 km southeast of JST). This indicates that titration is occurring across the city, and that EQUATES does not capture titration because of systematic biases in modeled O_3 and/or NO, as the phenomenon is not a localized event, and this should be captured in the model.

Biases in modeled $[O_3]$ and [NO] may be related to an overestimation of NBL height, leading to an over dilution of NO. As seen in other CMAQ-based studies in the region (Skipper et al., 2024), CO, a tracer for dilution, has consistently lower concentrations in the model at SDK by ∼100 ppbv across 2011–2019. Modeled CO decreases throughout the night while observations increase. This may also cause part of the underestimate in nighttime VOC concentrations (Figure S6 in Supporting Information S1). Since aged organic aerosol concentrations increase with BLH in the SE US due to downward mixing from aloft, a high bias in nocturnal aerosol concentrations in CMAQ compared to observations in prior studies also supports the overestimate in NBL (Chen et al., 2021).

Additionally, parameterizations of dry deposition in CMAQ may create biases in nighttime $[O_3]$, in which the SE US is especially sensitive (Baublitz et al., 2020). The Surface Tiled Aerosol and Gas Exchange (STAGE) module is used to model dry deposition in EQUATES. During the summer, STAGE produces slower O_3 deposition velocities in the Eastern US than its counterpart scheme, the M3Dry module (Hogrefe et al., 2023). This leads to slightly higher (up to 1 ppbv) predicted $[O_3]$ when using STAGE, which may contribute to the overall high bias of nighttime concentrations in the model. Since there is higher dry deposition over more vegetated areas, and CMAQ consistently underpredicts nighttime biogenic concentrations in the urban SE US (Figure 4b, Figures S2a and S6 in Supporting Information S1), O_3 deposition may be underestimated.

3.2. The Relative Importance of NO_3 for Monoterpene Oxidation

Nitrate radical abundance, and therefore F_{NO3}, is determined both by PNO_3 and the NO_3 loss rate, which is mostly driven by [MT] and [NO] at night. Figure 3 shows calculated steady-state nighttime $[NO_3]$, and observed [MT]

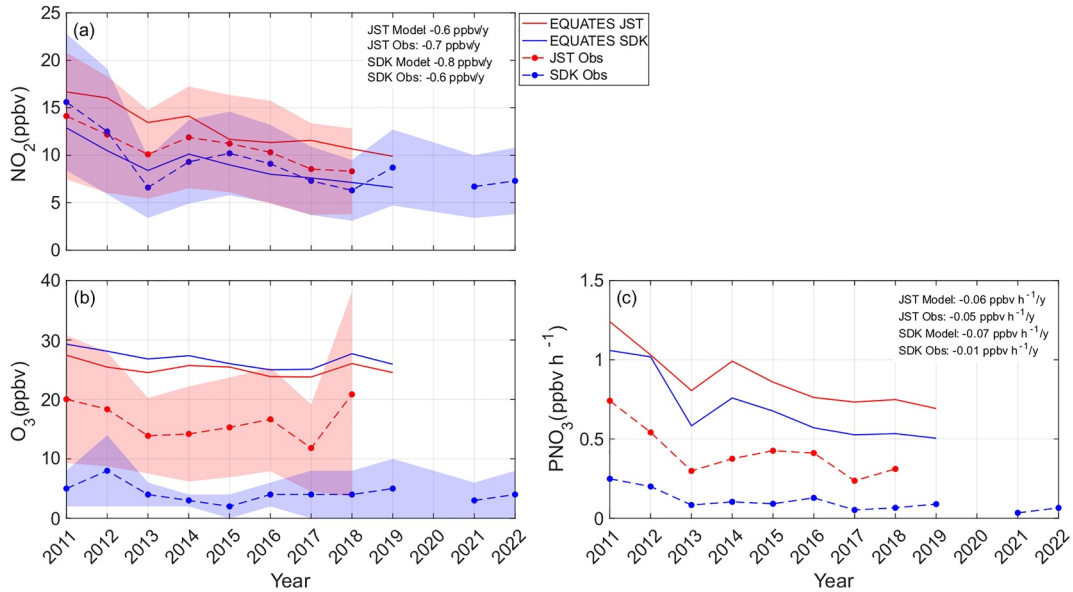

Figure 2. Annual median summertime (JJA) nocturnal (21:00–06:00 LT) observed (dashed) and modeled surface (solid) NO_2 (ppbv) (a), O_3 (ppbv) (b), and calculated PNO_3 (ppbv h^{-1}) (c) at SDK (blue) and JST (red) from 2011 to 2022. Shaded error bars represent the median absolute deviation (MAD) for observations. Statistically significant trends calculated from a linear regression model are included for NO_2 and PNO_3.

and [NO]. Despite large differences in calculated PNO_3 between the two sites (Figure 2) [NO_3] shows little spatial gradient, with median NO_3 at JST = 0.11 pptv and SDK = 0.081 pptv. Higher NO and NO + NO_3 reaction rates at JST offset the high PNO_3. [MT] is higher at SDK than JST, likely reflecting higher local biogenic emissions. Temperatures, and therefore emission rates, are not significantly different between years. As a result, total MT

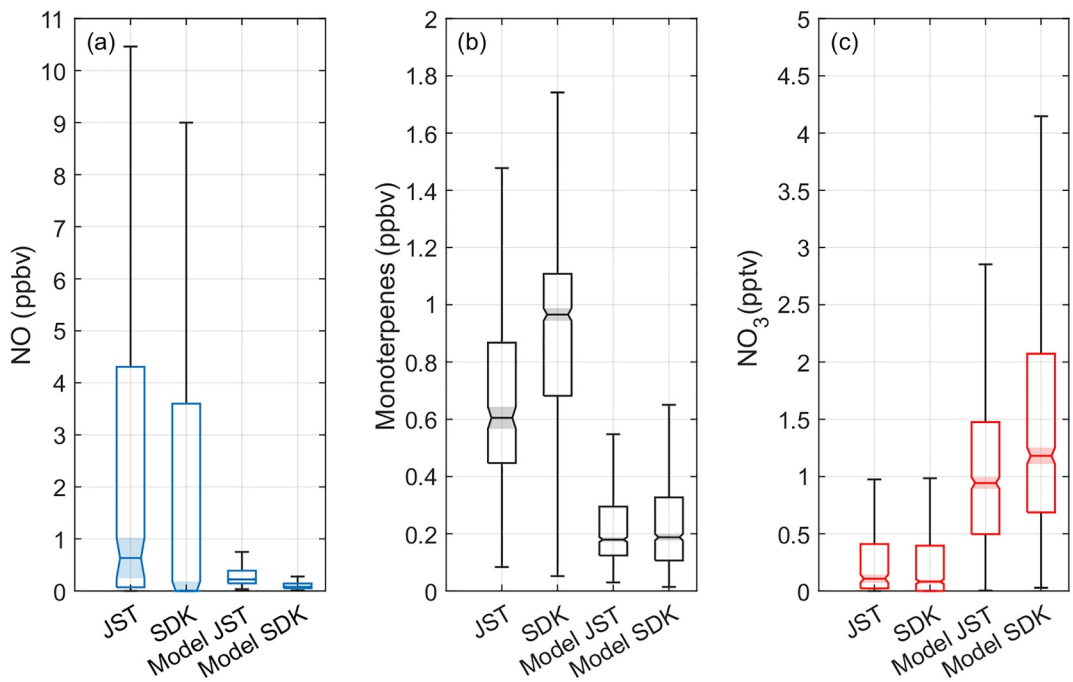

Figure 3. Box and whisker plots of nighttime (21:00–06:00 LT) NO (a), MT (b), and NO_3 (c) concentrations (ppbv) at JST 2017, SDK 2022, and EQUATES outputs at JST and SDK 2017. The shaded areas of the box plots represent notches for median values. Box plots whose notches do not overlap have statistically different medians ($p < 0.05$) between sites.

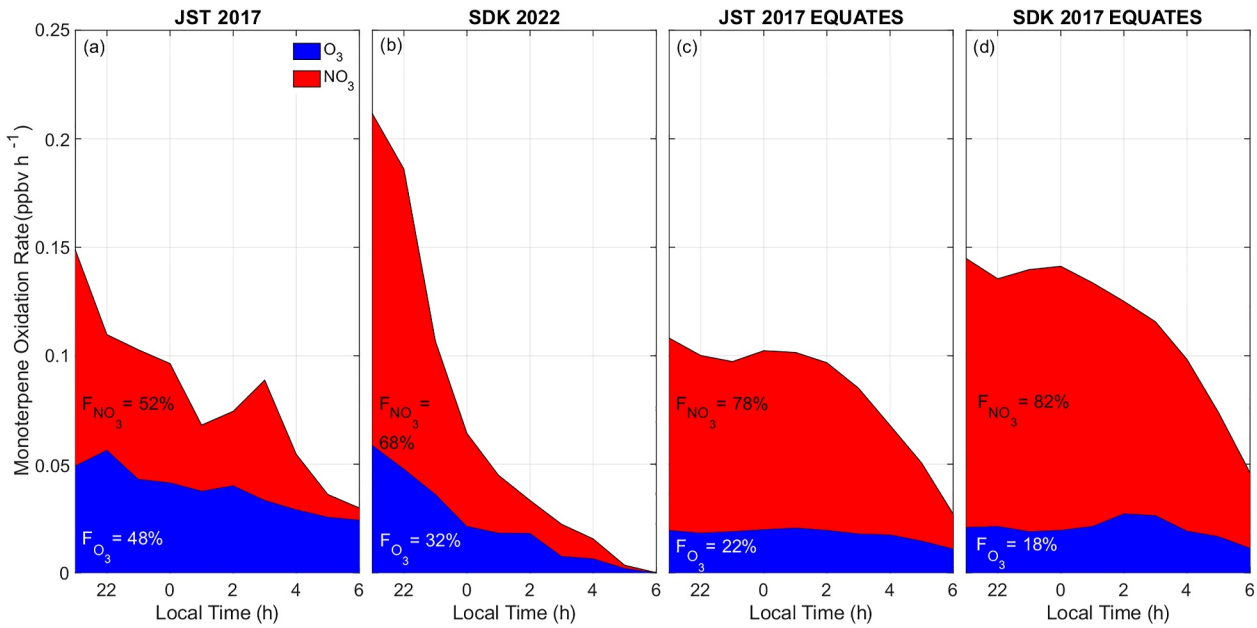

Figure 4. Median summertime (JJA) nighttime (21:00–06:00 LT) diurnal cycle of MT oxidation rates (ppbv h^{-1}) attributable to NO_3 (blue) and O_3 (red) for observations in 2017 JST (a), 2021 SDK (b), and modeled in 2017 JST (c) and SDK (d).

oxidation is faster at SDK. Figure 4 shows median F_{NO3} and MT oxidation rates at the two locations over all nighttime hours. NO_3 is the dominant MT nighttime oxidant at both sites (F_{NO3} = 52% and 68% for JST 2017 and SDK 2022, respectively). While [MT] is constant, MT oxidation rates decrease through the night alongside oxidant concentrations. In Figure 4a, the increase in F_{NO3} between 02:00–03:00 LT is indicative of an increase in [NO_3] during that time, which is attributed to the NO_3 + NO and NO_3 + BVOC sinks decreasing at a faster rate than PNO_3.

While NO_x emissions are highest in the urban core, trends and variability in early evening suburban oxidant concentrations are likely to have a larger relative impact on observed oxidation products.

Figures 4 and 5 also demonstrate the limitations of model-based assessments of nighttime surface-level VOC oxidation. EQUATES consistently and significantly underpredicts both [MT] and [NO] in 2017 (Normalized Mean Bias (NMB) = −70% and −92%, respectively). Combined with the overestimate in PNO_3, the net result is a high bias in [NO_3] (NMB = 232%). While both oxidants are overestimated in EQUATES, the relative impact for NO_3 is higher, creating a positive bias in F_{NO3}. In 2017, median EQUATES F_{NO3} = 78% at JST and 82% at SDK. While observations show a continual decrease in MT oxidation rates over the course of the night, modeled F_{NO3} remains flat until ~01:00 LT before declining due to a decrease in [O_3] and thus [NO_3], which inhibits NO_3 + MT. The similarity between sites can be mapped to similarity in modeled [O_3] (Figure 2), as NO + O_3 titration is not well captured. As in the observations, modeled MT oxidative rates are faster at SDK compared to JST, despite the higher PNO_3 at SDK. While EQUATES F_{NO3} is larger than the observed F_{NO3}, total MT + NO_3 loss rate is significantly underestimated at both sites due to low [MT], and the production of MT + NO_3 products is likely also underrepresented. In the daylight hours, NO_3 contribution to monoterpene oxidation is likely negligible. In 2019, median daytime (7–20 LT) [NO_3] in EQUATES is 0.3 pptv at both JST and SDK, and F_{NO3} (considering F_{OH}, as well) is 3%.

With these limitations in mind, we can examine the accuracy of the trends in modeled [NO_3] and F_{NO3}, which would influence trends in modeled oxidation products. As modeled [MT] shows little interannual variability (Figure S2a in Supporting Information S1), the NO_3 budget reflects trends in modeled [NO_x]. From 2013 to 2019, EQUATES [NO_3] is relatively constant: the decrease in modeled PNO_3 is matched by a decrease in NO + NO_3 (Figure S2b in Supporting Information S1). As a consequence of the model not capturing O_3 titration, dry deposition, and/or NBL, it likely misses an observed trend in MT oxidation products within a polluted urban

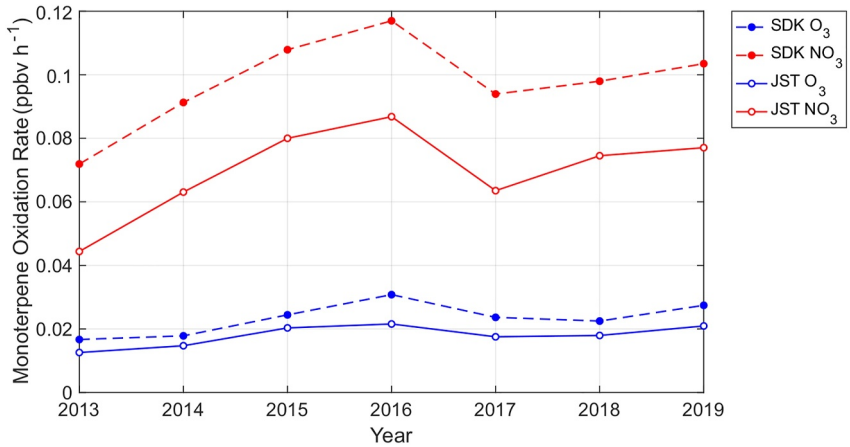

Figure 5. Annual median nighttime (21:00–06:00 LT) MT oxidation rates (ppbv h^{-1}) attributable to NO_3 (red) and O_3 (blue) from 2013 to 2019 at SDK (dashed) and JST (solid) calculated from EQUATES.

center. However, modeled OVOC trends may be more reflective of pristine locations with lower nighttime NO_x and higher [NO_3].

3.3. Differences in Aircraft-Based and Ground-Based Assessments of PNO_3

To demonstrate the differences between the urban NBL and regional residual layer chemistry on evaluations of PNO_3, we isolate JST observations and model outputs from the nights of 19 June and 02 July 2013, when SENEX flights took place, and focus on the same early evening hours (21:00–01:00 LT) (Figure 6). SDK measurements are not available on this night. At JST, surface-level [NO] is higher than SENEX observations, with a large standard deviation on 19 June indicative of fresh emission (Figure 6a). Surface-level [O_3] is consistently lower than in the residual layer (Figure S7 in Supporting Information S1), largely due to the NO + O_3 reaction (and therefore higher NO_2). The net result is a much lower PNO_3 in the residual layer (<0.2 ppbv hr^{-1} compared to 0.5–1.25 ppbv hr^{-1} in the NBL) (Figure 6d).

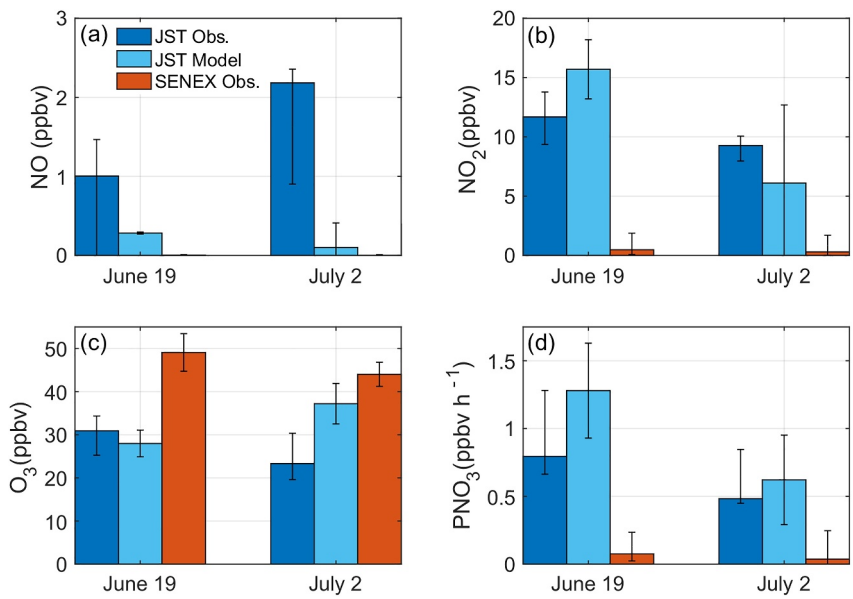

Figure 6. Median NO (a), NO_2 (b), O_3 (c), and calculated PNO_3 (d) of ground observations at JST (dark blue), first (surface) layer outputs from EQUATES at JST (light blue), and regional SENEX observations (red) from 21:00–01:00 LT on 19–20 June 2013 and 02–03 July 2013. Error bars represent MAD of hourly averages at JST observed and modeled, and MAD of 1 s resolution measurements during SENEX.

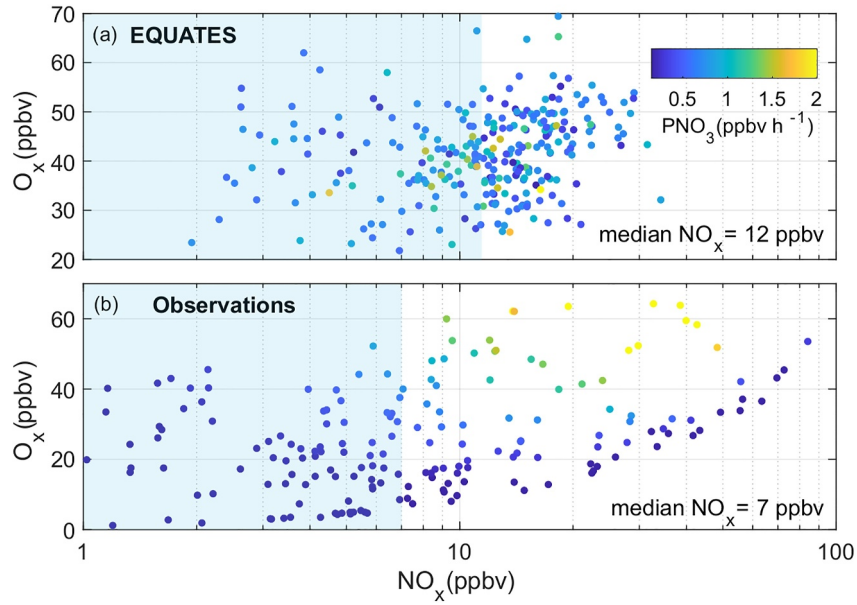

Figure 7. O_x (ppbv) as a function of NO_x (ppbv) colored by PNO_3 (ppbv) at 01:00 LT each night from 2017 to 2019 in EQUATES (a) and observations in 2017–2018 (b) at JST. The shaded blue regions represent [NO_x] less than the medians of each data set, 12.4 and 6.9 ppbv in the model and observations, respectively.

Edwards et al. (2017) calculated an F_{NO3} of 52% (19 June) and 55% (2 July) for regional BVOC loss on these two nights. These low calculated F_{NO3} values reflect consistently low PNO_3 and high O_3 in the residual layer. Another consideration is differences in BVOC composition between the residual layer and NBL. A three-fold decrease in nighttime [MT] was observed from the surface up to 1 km above ground level (agl) during SENEX due to the continual nocturnal emission of MT (Edwards et al., 2017). A similar vertical profile was found for isoprene, which accounted for >90% of total residual layer [BVOC] at sunset (Edwards et al., 2017). Since the residual layer is mainly comprised of isoprene and the NBL of MT, and because the MT + NO_3 rate constant is larger than that of isoprene + NO_3, oxidant importance and resultant product distributions may be influenced by BVOC gradients as well as oxidant vertical gradients. SENEX observations result in an O_3-centric view that may not reflect surface-level trends, but represent a comparatively larger volume of air and provide insight into the role of mixing in the observed surface-level concentrations of VOCs and their oxidation products in the early morning.

3.4. Influence of NO_x Reductions

We use O_x ([O_x] = [NO_2] + [O_3]) to quantify the effects of future NO_x emission reductions on oxidant relevance in a NO_x-sensitive regime like Atlanta. Although long-term regional declines in NO_x are expected to decrease total O_x, we find that in urban areas in the SE US, when nighttime [NO_x] is below the median value of 12.4 ppbv in the model, there are no further reductions in [O_x] (Figure 7a). O_x concentrations may still range from 20 to 60 ppbv in this regime, with no associated decrease in PNO_3, likely due to the lack of O_3 titration in the model. Above the median, the model shows a stronger relationship ($r = 0.39$) of declining [O_x] with [NO_x], reflecting the daytime relationship of increasing [O_3] with [NO_x].

In observations, we see similar correlation ($r = 0.34$) between [O_x] and [NO_x] when [NO_x] is above the median (6.9 ppbv) (Figure 7b), again reflective of the daytime relationship between O_3 and NO_x. Under this regime, PNO_3 decreases from ~2 to 1 ppbv hr^{-1}. Below the median NO_x value, we see a flattening of this positive relationship due to the contribution of background O_3 concentrations, and [O_x] still varies between 0 and 40 ppbv. As a result, we do not see the same magnitude in the gradient of PNO_3, with all values at or below ~0.5 ppbv hr^{-1}. Since we do not see a decline in PNO_3 under lower NO_x in both observations and EQUATES, we may expect constant [NO_3] or potentially a relative increase in concentrations in the future due to a reduced NO_3 + NO sink.

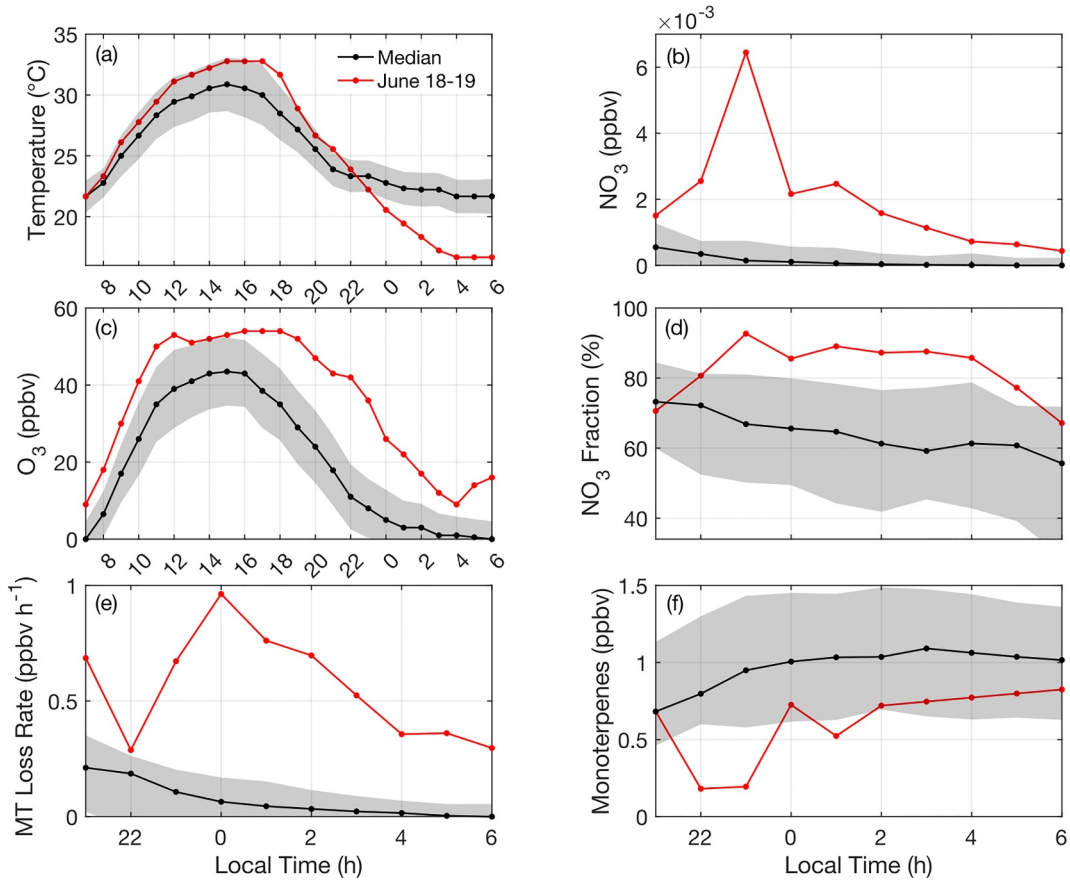

Figure 8. Median summertime (JJA) diurnal cycle (black) and 18–19 June extreme heat event comparison (red) at SDK of temperature (a), NO_3 (ppbv) (b), O_3 (ppbv) (c), NO_3 fractional contribution to MT loss (%) (d), total MT oxidation rate (ppbv h^{-1}) (e), and MT concentrations (f). Shaded error bars represent MAD.

Constant $[O_x]$ and smaller changes in PNO_3 under future NO_x reductions will likely result in a lack of change in F_{NO3}.

3.5. Influence of Heatwaves

Observations demonstrate how heatwaves increase MT oxidation rates and F_{NO3}. Daily maximum temperatures (15 LT) in summer 2022 at SDK are consistently associated with high daytime O_3 across the city (r = 0.82). Nights with $[O_3]$ 10 ppbv above the median have a daytime temperature 3°C above the median. We do not see a similar dependence in the model, where high daily maximum (15 LT) temperatures in summer 2019 are not associated with O_3 (r = 0.009), potentially due to an underestimate in biogenic emissions (Figure S6 in Supporting Information S1). Additionally, there is a notable interannual similarity between the number of heatwave days and O_x levels at both sites (Figure S3 in Supporting Information S1).

Measurements at SDK on 16–19 June illustrate the impact of the higher O_3 on calculated PNO_3 and F_{NO3}. During this extreme heat event, nighttime O_3 was more than twice the median value (Figure 8c). High O_3 increased PNO_3 to >11 times higher than median value $[NO_3]$ (Figure 8d) increased from 2 to 6 ppt, as [NO] remained low. F_{NO3} increased from 60%–70% to 70%–90% (Figure 8d). While MT emission rates are expected to increase under higher temperatures (Nagalingam et al., 2023), the high oxidant concentrations led to low observed [MT], at least 0.2 ppbv lower than the median (Figure 8f).

OVOC measurements during a separate heatwave event—which were not available at SDK—also showed increased MT oxidation rates, and demonstrated a larger relative importance of NO_3. Measurements on the night

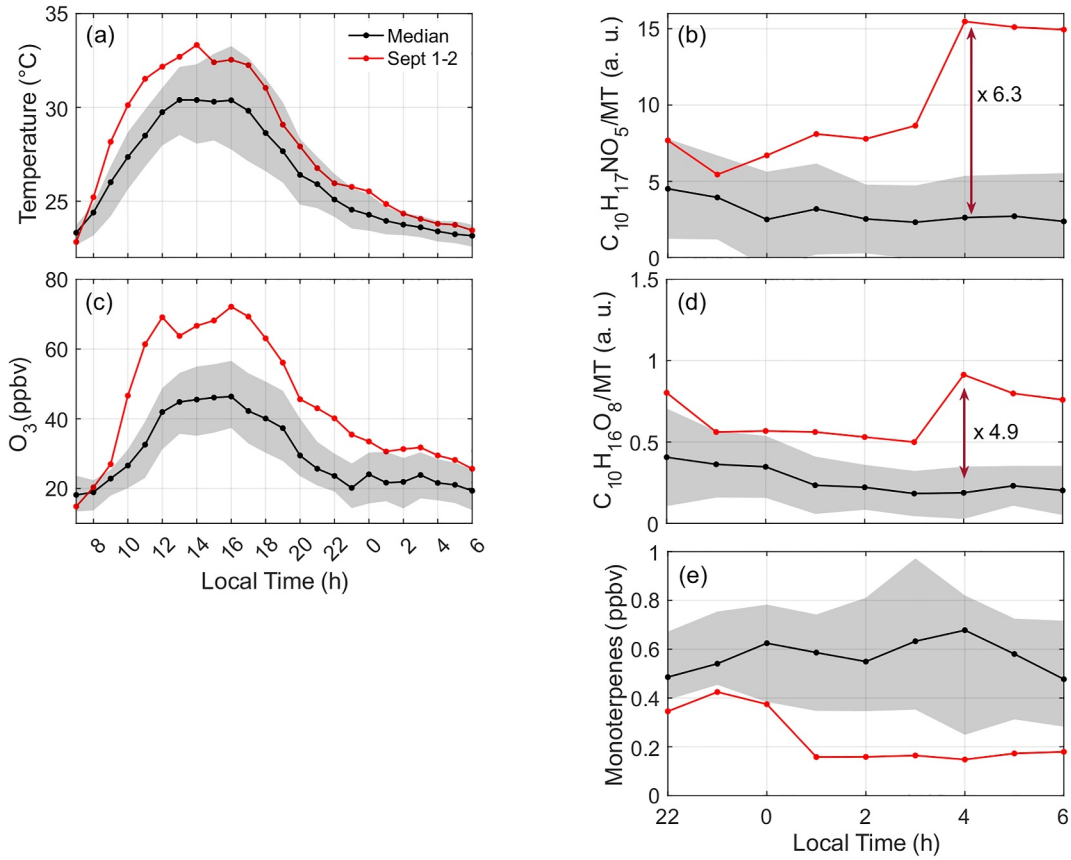

Figure 9. Median summertime (JJA) diurnal cycle (black) and 01–02 September extreme heat event comparison (red) at JST of temperature (a) ($C_{10}H_{17}NO_{5,g}$ + $C_{10}H_{17}NO_{5,p}$)/MT (arbitrary units) (b), O_3 (ppbv) (c) ($C_{10}H_{16}O_{8,g}$ + $C_{10}H_{16}O_{8,p}$)/MT (arbitrary units) (d), and MT (ppbv) concentrations (e). Shaded error bars represent MAD. $C_{10}H_{17}NO_5$ and $C_{10}H_{16}O_8$ represent summed gas- and particle-phase signals from the FIGAERO-CIMS.

of 01–02 September at JST show similarly high [O_3], low [NO], and elevated [NO_3]. The ratios of both MT + O_3 and MT + NO_3 oxidation products, $C_{10}H_{16}O_8$ and $C_{10}H_{17}NO_5$ respectively, are higher than median values over August–September (up to 4.9 and 6.3 times, respectively), with a greater relative increase in the gas + particle phase $C_{10}H_{17}NO_5$ to MT ratio (Figure 9b). Assuming similar lifetimes of $C_{10}H_{17}NO_5$ and $C_{10}H_{16}O_8$, the relative increase in $C_{10}H_{17}NO_5$/MT during the heatwave is consistent with an increase in F_{NO3}.

Our results suggest that in the SE US, MT lifetimes and F_{NO3} will remain constant as NO_x emissions decrease, but that this effect could be offset by a long-term increase in extreme heat events. Heatwaves are linked to higher nighttime O_3 and therefore O_x in the SE US. An increase in O_x derived from elevated O_3 decreases MT lifetimes (Figure 10). Although O_x and τ_{MT} share the same relationship in both observations and the model, the range of lifetimes varies more widely in the observations (0–30 hr) for [O_x] 10–50 ppbv. In the observational data set, when [O_x] > 25 ppbv, τ_{MT} is consistently less than 5 hr (Figure 10a). This agrees with EQUATES outputs, in which lifetimes remain below 5 hr for all [O_x] (Figure 10b). This is another result of the overestimation of [O_3] in the model. Since EQUATES predicts F_{NO3} to be >60% consistently, O_3 is never the dominant oxidant for MT loss in the model. This differs in the observational data set, in which lifetimes <5 hr still vary in oxidant contribution (30%–90% NO_3) (Figure 10a). On the nights of the heatwave however (16–19 June 2022), [O_x] varies between 20 and 35 ppbv across the four nights but F_{NO3} remains >80%.

An increase in F_{NO3} arises as τ_{MT} decreases under constant [O_x] in EQUATES (Figure 10b) and in observations (Figure 10a), but overall indicates that NO_3 increases in importance as MT oxidation rates increase. The gradient in F_{NO3} reflects the [NO_2]/[O_3] ratio, which is one factor that determines NO_3 abundance. PNO_3 scales with [O_x]^2 and quadratically with [NO_2]/[O_3] (Wang, Xi, et al., 2023). As described by Wang, Xi, et al. (2023), if the [NO_2]/

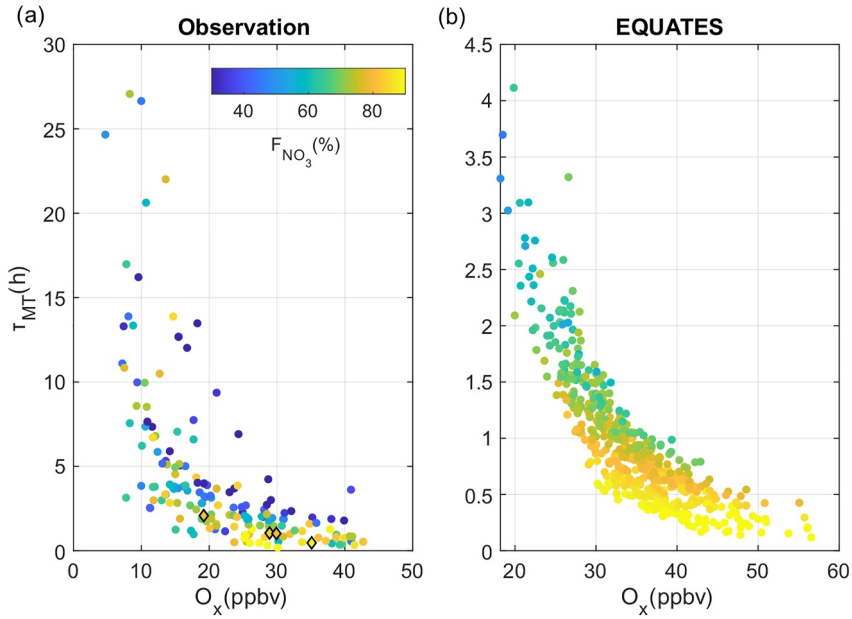

Figure 10. Total lifetime of MT (h) at 01:00 LT each night as a function of [O_x] (ppbv) colored by NO_3 fractional contribution to MT loss (%) for observations at JST in 2017, SDK in 2021–2022 (a) and EQUATES 2017–2019 at both sites (b). Heatwave nights from 16 to 19 June 2022 are denoted by diamonds in (a). Since there were no clear distinctions in the relationship between [O_x] and τ_{MT} between JST and SDK both observationally and within the model, we did not differentiate the data sets by location.

[O_3] ratio is < 1, PNO_3 will decrease with a decreasing ratio under constant O_x. If the ratio is > 1, PNO_3 will increase with a decreasing [NO_2]/[O_3]. Although further decreases in NO_x emission will have a shrinking impact on total O_x concentrations (Figure 7), the resultant decrease in the [NO_2]/[O_3] ratio will reduce PNO_3 and F_{NO3} if the ratio falls below 1 and continues to decline. During extreme heat events, the relative increase in [O_x] will result in high PNO_3 and F_{NO3}, despite the [NO_2]/[O_3] ratio being <1 under simultaneously lower NO_x and higher O_3 conditions.

Higher O_x will likely drive organic nitrate and aerosol production. An increased importance of NO_3 under lower [NO_x] and higher [O_3] may be uniformly experienced across an urban region, although the magnitude will likely differ within the urban core compared to the suburbs depending on their respective rates of NO_x decline. Consequently, despite efforts to reduce NO_x, at night we could continue to see high oxidative capacity for MT and formation of organic nitrates in the future. The contribution of MT + NO_3 and MT + O_3 to SOA formation depends on the aerosol yield and mass loading characteristic of a certain location. Xu, Guo, et al. (2015) estimated the SOA production resulting from NO_3 oxidation and ozonolysis of MT and isoprene for a rural site in Alabama and found that 64% of total nighttime OA production arises from the NO_3 oxidation pathway. If the same parameters hold true for urban areas in the region, we anticipate higher nocturnal MT-SOA with increased organic nitrate contribution during extreme heat events. We would not expect similar daytime trends since lower NO_x leads to a lower contribution of the RO_2 + NO pathway (which forms organic nitrates) compared to other RO_2 pathways (Brown et al., 2012).

Previous studies have shown that organic nitrates from MT + NO_3 contribute significantly to the less-oxidized oxygenated organic aerosol (LO-OOA) budget in the SE US (Xu, Guo, et al., 2015). The temperature dependence of LO-OOA at night from 15 to 25°C supports that organic nitrate formation increases under extreme heat events (Chen et al., 2020). This differs from outputs of the CAM6 model, in which an increase in MT emissions from 1988 to 2019 as a result of a warming climate predicts higher ozonolysis-derived SOA in the Eastern US (Liu et al., 2023). This discrepancy is likely due to a misrepresentation of NO_x reductions in the model.

There has been a decrease in summertime aerosol in the SE US (Liu et al., 2023). Our results suggest decreases in NO_3-initiated MT oxidation are likely not the cause for this decline. Under further anthropogenic emission

reductions, we do not anticipate a causal reduction in F_{NO3} or MT-derived organic nitrate production, but rather a lack of trend in the future. Across an urban area in the SE US, we typically see higher nighttime O_3 and PNO_3 within the urban core, which is not captured by EQUATES due to modeled biases in [O_3] and a lack of differences in [MT] with the urban background as a result of an underprediction in emission fluxes in both urban and suburban areas. This suggests higher F_{NO3} in the urban center compared to the surrounding suburban areas, but not necessarily higher OVOC and aerosol formation due to the limitations of [MT].

4. Conclusions

We demonstrate that NO_3 continues to dominate NBL MT loss in the greater Atlanta area (52%–68%). We suggest no decline in NO_3-initiated MT oxidation, which differs from previous studies that predicted the increasing importance of ozonolysis for BVOC loss at night in the SE US leading to a general reduction in organic nitrate aerosol (Edwards et al., 2017; Liu et al., 2023; Xu, Guo, et al., 2015). Despite modeling studies also suggesting a reduction in organic nitrate aerosol in the Eastern US (Liu et al., 2023), we find no trend in NO_3 importance for nocturnal MT loss in Atlanta. At JST, where the NO_3 + NO sink is presently larger, future NO_x emission reductions will play a more significant role within the urban core to further increase NO_3 concentrations and F_{NO3}.

Due to elevated [O_3] and reduced PNO_3 in the residual layer, aircraft observations provide a differing perspective on nighttime chemistry—one in which the relative importance of O_3 for BVOC oxidation is greater compared to the NBL. Differences in BVOC composition, with the residual layer comprising of mainly isoprene and the NBL of MT also lead to varying oxidation rates and oxidant importance. Additionally, higher [BVOC] in the NBL lead to greater loss rates than aloft, indicative of higher OVOC production. Higher winds in the residual layer compared to the NBL also allow for faster mixing, transport and dilution of pollutants. As such, the buildup of oxidants in the NBL also leads to increased nocturnal oxidation and SOA formation compared to the residual layer, indicating near-surface chemistry at night must be assessed separately. There remains a need for continued suburban to urban observations to monitor surface-level heterogeneity.

Increased O_3 from extreme heat events and lower NO_x may lead to higher F_{NO3} and total O_x, which is shown to be associated with shorter τ_{MT}. As a result, it may take longer for us to reach an O_3-dominated regime than previously expected. Upon further NO_x emission reductions, autoxidation and/or $RO_2 + RO_2$ reactions may play an increasingly important role in both day and nighttime VOC oxidation and SOA formation under warm conditions typical of summers in the SE US (Praske et al., 2018). As a result, low [NO] conditions may also relatively increase HOM production in the future (Molteni et al., 2019; Nie et al., 2023; Zhao et al., 2018).

EQUATES overestimates nighttime O_3 and underpredicts NO, leading to high biases in PNO_3 and O_x. The current biases in modeled O_x in the urban SE US are seen to play a role in determining the relationship between [NO_2]/[O_3] and estimating PNO_3 and F_{NO3}. Regional air quality models like CMAQ will need to better capture these parameters to effectively predict MT lifetimes and oxidation pathways at night.

Disclaimer

The views expressed in this article are those of the authors and do not necessarily reflect the views or polices of the U.S. EPA.

Data Availability Statement

The data from SDK PAMS are available at the EPA AQS API via https://aqs.epa.gov/aqsweb/documents/data_api.html. The SEARCH network data are available at https://www.dropbox.com/sh/o9hxoa4wlo97zpe/AACbm6LetQowrpUgX4vUxnoDa?dl=0. The NOAA P-3 aircraft measurements from SENEX are available at https://csl.noaa.gov/groups/csl7/measurements/2013senex/P3/DataDownload/. The JST measurements in 2017–2018, along with Georgia Tech rooftop data (O_3, NO, VOCs, OVOCs) from the summer 2022 field campaign, courtesy of the Ng and Kaiser Labs, are available at Github via https://github.com/KaiserLab-GeorgiaTech/NighttimeOxidationPaper/tree/v4 and archived at Zenodo (KaiserLab-GeorgiaTech, 2024). Meteorological parameters measured at Georgia Tech are available at WeatherSTEM via https://gatech.weatherstem.com/. Surface model outputs from EQUATES are available via https://www.epa.gov/cmaq/equates#how_to_download_

equates_data (US EPA, 2021). Reaction rate coefficients are available at the Master Chemical Mechanism v3.3.1 via www.mcm.york.ac.uk. Figures were made with MATLAB version 2021b, available under license at https://www.mathworks.com. The map was created using ArcGIS® software by Esri. ArcGIS® and ArcMap™ are the intellectual property of Esri and are used herein under license. Copyright © Esri. All rights reserved. For more information about Esri® software, please visit https://www.esri.com.

Acknowledgments
The authors thank Kristen Foley for providing comprehensive EQUATES outputs. The authors thank the Georgia Environmental Protection Division for collection, processing, and availability of data from the South DeKalb Photochemical Assessment Monitoring Site. The authors thank the SEARCH network personnel for collecting and providing data from the Jefferson Street site. This study was supported by the NOAA Climate Program Office's Atmospheric Chemistry, Carbon Cycle, and Climate program (grant NA21OAR4310221).

References

Appel, K. W., Bash, J. O., Fahey, K. M., Foley, K. M., Gilliam, R. C., Hogrefe, C., et al. (2021). The Community Multiscale Air Quality (CMAQ) model versions 5.3 and 5.3.1: System updates and evaluation. *Geoscientific Model Development*, *14*(5), 2867–2897. https://doi.org/10.5194/gmd-14-2867-2021

Ayres, B. R., Allen, H. M., Draper, D. C., Brown, S. S., Wild, R. J., Jimenez, J. L., et al. (2015). Organic nitrate aerosol formation via NO_3 + biogenic volatile organic compounds in the southeastern United States. *Atmospheric Chemistry and Physics*, *15*(23), 13377–13392. https://doi.org/10.5194/acp-15-13377-2015

Bash, J. O., Baker, K. R., & Beaver, M. R. (2016). Evaluation of improved land use and canopy representation in BEIS v3.61 with biogenic VOC measurements in California. *Geoscientific Model Development*, *9*(6), 2191–2207. https://doi.org/10.5194/gmd-9-2191-2016

Bates, K. H., Burke, G. J. P., Cope, J. D., & Nguyen, T. B. (2022). Secondary organic aerosol and organic nitrogen yields from the nitrate radical (NO_3) oxidation of alpha-pinene from various RO_2 fates. *Atmospheric Chemistry and Physics*, *22*(2), 1467–1482. https://doi.org/10.5194/acp-22-1467-2022

Baublitz, C. B., Fiore, A. M., Clifton, O. E., Mao, J., Li, J., Correa, G., et al. (2020). Sensitivity of tropospheric ozone over the southeast USA to dry deposition. *Geophysical Research Letters*, *47*(7), e2020GL087158. https://doi.org/10.1029/2020GL087158

Benish, S. E., Bash, J. O., Foley, K. M., Appel, K. W., Hogrefe, C., Gilliam, R., & Pouliot, G. (2022). Long-term regional trends of nitrogen and sulfur deposition in the United States from 2002 to 2017. *Atmospheric Chemistry and Physics*, *22*(19), 12749–12767. https://doi.org/10.5194/acp-22-12749-2022

Bergin, R. A., Harkey, M., Hoffman, A., Moore, R. H., Anderson, B., Beyersdorf, A., et al. (2022). Observation-based constraints on modeled aerosol surface area: Implications for heterogeneous chemistry. *Atmospheric Chemistry and Physics*, *22*(23), 15449–15468. https://doi.org/10.5194/acp-22-15449-2022

Bianchi, F., Kurtén, T., Riva, M., Mohr, C., Rissanen, M. P., Roldin, P., et al. (2019). Highly oxygenated organic molecules (HOM) from gas-phase autoxidation involving peroxy radicals: A key contributor to atmospheric aerosol. *Chemical Reviews*, *119*(6), 3472–3509. https://doi.org/10.1021/acs.chemrev.8b00395

Blanchard, C. L., & Hidy, G. M. (2018). Ozone response to emission reductions in the southeastern United States. *Atmospheric Chemistry and Physics*, *18*(11), 8183–8202. https://doi.org/10.5194/acp-18-8183-2018

Bloss, C., Wagner, V., Jenkin, M. E., Volkamer, R., Bloss, W. J., Lee, J. D., et al. (2005). Development of a detailed chemical mechanism (MCMv3.1) for the atmospheric oxidation of aromatic hydrocarbons. *Atmospheric Chemistry and Physics*, *5*(3), 641–664. https://doi.org/10.5194/acp-5-641-2005

Boyd, C. M., Sanchez, J., Xu, L., Eugene, A. J., Nah, T., Tuet, W. Y., et al. (2015). Secondary organic aerosol formation from the β-pinene+NO_3 system: Effect of humidity and peroxy radical fate. *Atmospheric Chemistry and Physics*, *15*(13), 7497–7522. https://doi.org/10.5194/acp-15-7497-2015

Brown, S. S., Dubé, W. P., Bahreini, R., Middlebrook, A. M., Brock, C. A., Warneke, C., et al. (2013). Biogenic VOC oxidation and organic aerosol formation in an urban nocturnal boundary layer: Aircraft vertical profiles in Houston, TX. *Atmospheric Chemistry and Physics*, *13*(22), 11317–11337. https://doi.org/10.5194/acp-13-11317-2013

Brown, S. S., Dubé, W. P., Karamchandani, P., Yarwood, G., Peischl, J., Ryerson, T. B., et al. (2012). Effects of NO_x control and plume mixing on nighttime chemical processing of plumes from coal-fired power plants. *Journal of Geophysical Research*, *117*(D7). https://doi.org/10.1029/2011JD016954

Brown, S. S., Dubé, W. P., Osthoff, H. D., Wolfe, D. E., Angevine, W. M., & Ravishankara, A. R. (2007). High resolution vertical distributions of NO_3 and N_2O_5 through the nocturnal boundary layer. *Atmospheric Chemistry and Physics*, *7*(1), 139–149. https://doi.org/10.5194/acp-7-139-2007

Brown, S. S., Dubé, W. P., Peischl, J., Ryerson, T. B., Atlas, E., Warneke, C., et al. (2011). Budgets for nocturnal VOC oxidation by nitrate radicals aloft during the 2006 Texas Air Quality Study. *Journal of Geophysical Research*, *116*(D24). https://doi.org/10.1029/2011JD016544

Brown, S. S., Neuman, J. A., Ryerson, T. B., Trainer, M., Dubé, W. P., Holloway, J. S., et al. (2006). Nocturnal odd-oxygen budget and its implications for ozone loss in the lower troposphere. *Geophysical Research Letters*, *33*(8). https://doi.org/10.1029/2006GL025900

Brown, S. S., & Stutz, J. (2012). Nighttime radical observations and chemistry. *Chemical Society Reviews*, *41*(19), 6405–6447. https://doi.org/10.1039/C2CS35181A

Chen, X., Wang, H., Liu, Y., Su, R., Wang, H., Lou, S., & Lu, K. (2019). Spatial characteristics of the nighttime oxidation capacity in the Yangtze River Delta, China. *Atmospheric Environment*, *208*, 150–157. https://doi.org/10.1016/j.atmosenv.2019.04.012

Chen, Y., Guo, H., Nah, T., Tanner, D. J., Sullivan, A. P., Takeuchi, M., et al. (2021). Low-molecular-weight carboxylic acids in the southeastern U.S.: Formation, partitioning, and implications for organic aerosol aging. *Environmental Science and Technology*, *55*(10), 6688–6699. https://doi.org/10.1021/acs.est.1c01413

Chen, Y., Takeuchi, M., Nah, T., Xu, L., Canagaratna, M. R., Stark, H., et al. (2020). Chemical characterization of secondary organic aerosol at a rural site in the southeastern US: Insights from simultaneous high-resolution time-of-flight aerosol mass spectrometer (HR-ToF-AMS) and FIGAERO chemical ionization mass spectrometer (CIMS) measurements. *Atmospheric Chemistry and Physics*, *20*(14), 8421–8440. https://doi.org/10.5194/acp-20-8421-2020

Edwards, P. M., Aikin, K. C., Dube, W. P., Fry, J. L., Gilman, J. B., de Gouw, J. A., et al. (2017). Transition from high-to low-NO_x control of night-time oxidation in the southeastern US. *Nature Geoscience*, *10*(7), 490–495. https://doi.org/10.1038/ngeo2976

Fiore, A. M., Dentener, F. J., Wild, O., Cuvelier, C., Schultz, M. G., Hess, P., et al. (2009). Multimodel estimates of intercontinental source-receptor relationships for ozone pollution. *Journal of Geophysical Research*, *114*(D4). https://doi.org/10.1029/2008JD010816

Fischer, E. M., Beyerle, U., & Knutti, R. (2013). Robust spatially aggregated projections of climate extremes. *Nature Climate Change*, *3*(12), 1033–1038. https://doi.org/10.1038/nclimate2051

Foley, K. M., Pouliot, G. A., Eyth, A., Aldridge, M. F., Allen, C., Appel, K. W., et al. (2023). 2002–2017 anthropogenic emissions data for air quality modeling over the United States. *Data in Brief*, *47*, 109022. https://doi.org/10.1016/j.dib.2023.109022

Fry, J. L., Draper, D. C., Barsanti, K. C., Smith, J. N., Ortega, J., Winkler, P. M., et al. (2014). Secondary organic aerosol formation and organic nitrate yield from NO3 oxidation of biogenic hydrocarbons. *Environmental Science and Technology*, *48*(20), 11944–11953. https://doi.org/10.1021/es502204x

Fry, J. L., Kiendler-Scharr, A., Rollins, A. W., Wooldridge, P. J., Brown, S. S., Fuchs, H., et al. (2009). Organic nitrate and secondary organic aerosol yield from NO_3 oxidation of β-pinene evaluated using a gas-phase kinetics/aerosol partitioning model. *Atmospheric Chemistry and Physics*, *9*(4), 1431–1449. https://doi.org/10.5194/acp-9-1431-2009

Hansen, D. A., Edgerton, E., Hartsell, B., Jansen, J., Burge, H., Koutrakis, P., et al. (2006). Air quality measurements for the aerosol research and inhalation epidemiology study. *Journal of the Air and Waste Management Association*, *56*(10), 1445–1458. https://doi.org/10.1080/10473289.2006.10464549

Hansen, D. A., Edgerton, E. S., Hartsell, B. E., Jansen, J. J., Kandasamy, N., Hidy, G. M., & Blanchard, C. L. (2003). The southeastern aerosol research and characterization study: Part 1—Overview. *Journal of the Air and Waste Management Association*, *53*(12), 1460–1471. https://doi.org/10.1080/10473289.2003.10466318

Haslett, S. L., Bell, D. M., Kumar, V., Slowik, J. G., Wang, D. S., Mishra, S., et al. (2023). Nighttime NO emissions strongly suppress chlorine and nitrate radical formation during the winter in Delhi. *Atmospheric Chemistry and Physics*, *23*(16), 9023–9036. https://doi.org/10.5194/acp-23-9023-2023

Hogrefe, C., Bash, J. O., Pleim, J. E., Schwede, D. B., Gilliam, R. C., Foley, K. M., et al. (2023). An analysis of CMAQ gas-phase dry deposition over North America through grid-scale and land-use-specific diagnostics in the context of AQMEII4. *Atmospheric Chemistry and Physics*, *23*(14), 8119–8147. https://doi.org/10.5194/acp-23-8119-2023

Jenkin, M. E., Saunders, S. M., & Pilling, M. J. (1997). The tropospheric degradation of volatile organic compounds: A protocol for mechanism development. *Atmospheric Environment*, *31*(1), 81–104. https://doi.org/10.1016/S1352-2310(96)00105-7

Jenkin, M. E., Saunders, S. M., Wagner, V., & Pilling, M. J. (2003). Protocol for the development of the Master Chemical Mechanism, MCM v3 (Part B): Tropospheric degradation of aromatic volatile organic compounds. *Atmospheric Chemistry and Physics*, *3*(1), 181–193. https://doi.org/10.5194/acp-3-181-2003

Jenkin, M. E., Young, J. C., & Rickard, A. R. (2015). The MCM v3.3.1 degradation scheme for isoprene. *Atmospheric Chemistry and Physics*, *15*(20), 11433–11459. https://doi.org/10.5194/acp-15-11433-2015

KaiserLab-GeorgiaTech. (2024). KaiserLab-GeorgiaTech/NighttimeOxidationPaper: Added JST 2017-2018 data (version v4) [Dataset]. *Zenodo*. https://doi.org/10.5281/zenodo.11226303

Kim, P. S., Jacob, D. J., Fisher, J. A., Travis, K., Yu, K., Zhu, L., et al. (2015). Sources, seasonality, and trends of southeast US aerosol: An integrated analysis of surface, aircraft, and satellite observations with the GEOS-Chem chemical transport model. *Atmospheric Chemistry and Physics*, *15*(18), 10411–10433. https://doi.org/10.5194/acp-15-10411-2015

Lambe, A. T., Bai, B., Takeuchi, M., Orwat, N., Zimmerman, P. M., Alton, M. W., et al. (2023). Technical note: Gas-phase nitrate radical generation via irradiation of aerated ceric ammonium nitrate mixtures. *Atmospheric Chemistry and Physics*, *23*(21), 13869–13882. https://doi.org/10.5194/acp-23-13869-2023

Li, J., Mao, J., Fiore, A. M., Cohen, R. C., Crounse, J. D., Teng, A. P., et al. (2018). Decadal changes in summertime reactive oxidized nitrogen and surface ozone over the southeast United States. *Atmospheric Chemistry and Physics*, *18*(3), 2341–2361. https://doi.org/10.5194/acp-18-2341-2018

Liu, Y., Dong, X., Emmons, L. K., Jo, D. S., Liu, Y., Shrivastava, M., et al. (2023). Exploring the factors controlling the long-term trend (1988–2019) of surface organic aerosols in the continental United States by simulations. *Journal of Geophysical Research: Atmospheres*, *128*(9), e2022JD037935. https://doi.org/10.1029/2022JD037935

Luecken, D. J., Yarwood, G., & Hutzell, W. T. (2019). Multipollutant modeling of ozone, reactive nitrogen and HAPs across the continental US with CMAQ-CB6. *Atmospheric Environment*, *201*, 62–72. https://doi.org/10.1016/j.atmosenv.2018.11.060

Makar, P. A., Staebler, R. M., Akingunola, A., Zhang, J., McLinden, C., Kharol, S. K., et al. (2017). The effects of forest canopy shading and turbulence on boundary layer ozone. *Nature Communications*, *8*(1), 15243. https://doi.org/10.1038/ncomms15243

Molteni, U., Simon, M., Heinritzi, M., Hoyle, C. R., Bernhammer, A.-K., Bianchi, F., et al. (2019). Formation of highly oxygenated organic molecules from α-pinene ozonolysis: Chemical characteristics, mechanism, and kinetic model development. *ACS Earth and Space Chemistry*, *3*(5), 873–883. https://doi.org/10.1021/acsearthspacechem.9b00035

Nagalingam, S., Seco, R., Kim, S., & Guenther, A. (2023). Heat stress strongly induces monoterpene emissions in some plants with specialized terpenoid storage structures. *Agricultural and Forest Meteorology*, *333*, 109400. https://doi.org/10.1016/j.agrformet.2023.109400

Nah, T., Sanchez, J., Boyd, C. M., & Ng, N. L. (2016). Photochemical aging of α-pinene and β-pinene secondary organic aerosol formed from nitrate radical oxidation. *Environmental Science and Technology*, *50*(1), 222–231. https://doi.org/10.1021/acs.est.5b04594

Nie, W., Yan, C., Yang, L., Roldin, P., Liu, Y., Vogel, A. L., et al. (2023). NO at low concentration can enhance the formation of highly oxygenated biogenic molecules in the atmosphere. *Nature Communications*, *14*(1), 3347. https://doi.org/10.1038/s41467-023-39066-4

Peng, Y., Mouat, A. P., Hu, Y., Li, M., McDonald, B. C., & Kaiser, J. (2022). Source appointment of volatile organic compounds and evaluation of anthropogenic monoterpene emission estimates in Atlanta, Georgia. *Atmospheric Environment*, *288*, 119324. https://doi.org/10.1016/j.atmosenv.2022.119324

Pollack, I. B., Lerner, B. M., & Ryerson, T. B. (2010). Evaluation of ultraviolet light-emitting diodes for detection of atmospheric NO_2 by photolysis—Chemiluminescence. *Journal of Atmospheric Chemistry*, *65*(2), 111–125. https://doi.org/10.1007/s10874-011-9184-3

Praske, E., Otkjær, R. V., Crounse, J. D., Hethcox, J. C., Stoltz, B. M., Kjaergaard, H. G., & Wennberg, P. O. (2018). Atmospheric autoxidation is increasingly important in urban and suburban North America. *Proceedings of the National Academy of Sciences*, *115*(1), 64–69. https://doi.org/10.1073/pnas.1715540115

Pye, H. O. T., D'Ambro, E. L., Lee, B. H., Schobesberger, S., Takeuchi, M., Zhao, Y., et al. (2019). Anthropogenic enhancements to production of highly oxygenated molecules from autoxidation. *Proceedings of the National Academy of Sciences*, *116*(14), 6641–6646. https://doi.org/10.1073/pnas.1810774116

Rattanavaraha, W., Canagaratna, M. R., Budisulistiorini, S. H., Croteau, P. L., Baumann, K., Canonaco, F., et al. (2017). Source apportionment of submicron organic aerosol collected from Atlanta, Georgia, during 2014–2015 using the aerosol chemical speciation monitor (ACSM). *Atmospheric Environment*, *167*, 389–402. https://doi.org/10.1016/j.atmosenv.2017.07.055

Ravishankara, A. R. (1997). Heterogeneous and multiphase chemistry in the troposphere. *Science*, *276*(5315), 1058–1065. https://doi.org/10.1126/science.276.5315.1058

Reed, C., Evans, M. J., Di Carlo, P., Lee, J. D., & Carpenter, L. J. (2016). Interferences in photolytic NO_2 measurements: Explanation for an apparent missing oxidant? *Atmospheric Chemistry and Physics*, *16*(7), 4707–4724. https://doi.org/10.5194/acp-16-4707-2016

Ren, X., Harder, H., Martinez, M., Lesher, R. L., Oliger, A., Simpas, J. B., et al. (2003). OH and HO_2 chemistry in the urban atmosphere of New York City. *Atmospheric Environment*, *37*(26), 3639–3651. https://doi.org/10.1016/S1352-2310(03)00459-X

Riemer, N., Vogel, H., Vogel, B., Schell, B., Ackermann, I., Kessler, C., & Hass, H. (2003). Impact of the heterogeneous hydrolysis of N_2O_5 on chemistry and nitrate aerosol formation in the lower troposphere under photosmog conditions. *Journal of Geophysical Research*, *108*(D4). https://doi.org/10.1029/2002JD002436

Ryerson, T. B., Huey, L. G., Knapp, K., Neuman, J. A., Parrish, D. D., Sueper, D. T., & Fehsenfeld, F. C. (1999). Design and initial characterization of an inlet for gas-phase NO_y measurements from aircraft. *Journal of Geophysical Research*, *104*(D5), 5483–5492. https://doi.org/10.1029/1998JD100087

Ryerson, T. B., Williams, E. J., & Fehsenfeld, F. C. (2000). An efficient photolysis system for fast-response NO_2 measurements. *Journal of Geophysical Research*, *105*(D21), 26447–26461. https://doi.org/10.1029/2000JD900389

Saunders, S. M., Jenkin, M. E., Derwent, R. G., & Pilling, M. J. (2003). Protocol for the development of the Master Chemical Mechanism, MCM v3 (Part A): Tropospheric degradation of non-aromatic volatile organic compounds. *Atmospheric Chemistry and Physics*, *3*(1), 161–180. https://doi.org/10.5194/acp-3-161-2003

Silvern, R. F., Jacob, D. J., Mickley, L. J., Sulprizio, M. P., Travis, K. R., Marais, E. A., et al. (2019). Using satellite observations of tropospheric NO_2 columns to infer long-term trends in US NO_x emissions: The importance of accounting for the free tropospheric NO_2 background. *Atmospheric Chemistry and Physics*, *19*(13), 8863–8878. https://doi.org/10.5194/acp-19-8863-2019

Skipper, T. N., D'Ambro, E. L., Wiser, F. C., McNeill, V. F., Schwantes, R. H., Henderson, B. H., et al. (2024). Role of chemical production and depositional losses on formaldehyde in the community regional atmospheric chemistry multiphase mechanism (CRACMM). *EGUsphere*, 1–34. https://doi.org/10.5194/egusphere-2024-1680

Stutz, J., Alicke, B., Ackermann, R., Geyer, A., White, A., & Williams, E. (2004). Vertical profiles of NO_3, N_2O_5, O_3, and NO_x in the nocturnal boundary layer: 1. Observations during the Texas air quality study 2000. *Journal of Geophysical Research*, *109*(D12). https://doi.org/10.1029/2003JD004209

Stutz, J., Wong, K. W., Lawrence, L., Ziemba, L., Flynn, J. H., Rappenglück, B., & Lefer, B. (2010). Nocturnal NO_3 radical chemistry in Houston, TX. *Atmospheric Environment*, *44*(33), 4099–4106. https://doi.org/10.1016/j.atmosenv.2009.03.004

Takeuchi, M., & Ng, N. L. (2019). Chemical composition and hydrolysis of organic nitrate aerosol formed from hydroxyl and nitrate radical oxidation of α-pinene and β-pinene. *Atmospheric Chemistry and Physics*, *19*(19), 12749–12766. https://doi.org/10.5194/acp-19-12749-2019

US EPA. (2021). EQUATESv1.0: Emissions, WRF/MCIP, CMAQv5.3.2 data -- 2002-2019 US_12km and NHEMI_108km (version v5) [Dataset]. *UNC Dataverse*. https://doi.org/10.15139/S3/F2KJSK

Vose, R. S., Easterling, D. R., Kunkel, K. E., LeGrande, A. N., & Wehner, M. F. (2017). Temperature changes in the United States. https://doi.org/10.7930/J0N29V45

Wang, H., Wang, H., Lu, X., Lu, K., Zhang, L., Tham, Y. J., et al. (2023). Increased night-time oxidation over China despite widespread decrease across the globe. *Nature Geoscience*, *16*(3), 217–223. https://doi.org/10.1038/s41561-022-01122-x

Wang, Y., Xi, S., Zhao, F., Huey, L. G., & Zhu, T. (2023). Decreasing production and potential urban explosion of nighttime nitrate radicals amid emission reduction efforts. *Environmental Science and Technology*, *57*(50), 21306–21312. https://doi.org/10.1021/acs.est.3c09259

Warneke, C., Trainer, M., de Gouw, J. A., Parrish, D. D., Fahey, D. W., Ravishankara, A. R., et al. (2016). Instrumentation and measurement strategy for the NOAA SENEX aircraft campaign as part of the Southeast Atmosphere Study 2013. *Atmospheric Measurement Techniques*, *9*(7), 3063–3093. https://doi.org/10.5194/amt-9-3063-2016

Xu, L., Guo, H., Boyd, C. M., Klein, M., Bougiatioti, A., Cerully, K. M., et al. (2015). Effects of anthropogenic emissions on aerosol formation from isoprene and monoterpenes in the southeastern United States. *Proceedings of the National Academy of Sciences*, *112*(1), 37–42. https://doi.org/10.1073/pnas.1417609112

Xu, L., Pye, H. O. T., He, J., Chen, Y., Murphy, B. N., & Ng, N. L. (2018). Experimental and model estimates of the contributions from biogenic monoterpenes and sesquiterpenes to secondary organic aerosol in the southeastern United States. *Atmospheric Chemistry and Physics*, *18*(17), 12613–12637. https://doi.org/10.5194/acp-18-12613-2018

Xu, L., Suresh, S., Guo, H., Weber, R. J., & Ng, N. L. (2015). Aerosol characterization over the southeastern United States using high-resolution aerosol mass spectrometry: Spatial and seasonal variation of aerosol composition and sources with a focus on organic nitrates. *Atmospheric Chemistry and Physics*, *15*(13), 7307–7336. https://doi.org/10.5194/acp-15-7307-2015

Yu, K., Jacob, D. J., Fisher, J. A., Kim, P. S., Marais, E. A., Miller, C. C., et al. (2016). Sensitivity to grid resolution in the ability of a chemical transport model to simulate observed oxidant chemistry under high-isoprene conditions. *Atmospheric Chemistry and Physics*, *16*(7), 4369–4378. https://doi.org/10.5194/acp-16-4369-2016

Zhang, H., Yee, L. D., Lee, B. H., Curtis, M. P., Worton, D. R., Isaacman-VanWertz, G., et al. (2018). Monoterpenes are the largest source of summertime organic aerosol in the southeastern United States. *Proceedings of the National Academy of Sciences*, *115*(9), 2038–2043. https://doi.org/10.1073/pnas.1717513115

Zhao, Y., Thornton, J. A., & Pye, H. O. T. (2018). Quantitative constraints on autoxidation and dimer formation from direct probing of monoterpene-derived peroxy radical chemistry. *Proceedings of the National Academy of Sciences*, *115*(48), 12142–12147. https://doi.org/10.1073/pnas.1812147115

References From the Supporting Information

Kumar, V., Slowik, J. G., Baltensperger, U., Prevot, A. S. H., & Bell, D. M. (2023). Time-resolved molecular characterization of secondary organic aerosol formed from OH and NO_3 radical initiated oxidation of a mixture of aromatic precursors. *Environmental Science and Technology*, *57*(31), 11572–11582. https://doi.org/10.1021/acs.est.3c00225

Stanimirova, I., Rich, D. Q., Russell, A. G., & Hopke, P. K. (2023). A long-term, dispersion normalized PMF source apportionment of PM2.5 in Atlanta from 2005 to 2019. *Atmospheric Environment*, *312*, 120027. https://doi.org/10.1016/j.atmosenv.2023.120027

Toma, S., Bertman, S., Groff, C., Xiong, F., Shepson, P. B., Romer, P., et al. (2019). Importance of biogenic volatile organic compounds to acyl peroxy nitrates (APN) production in the southeastern US during SOAS 2013. *Atmospheric Chemistry and Physics*, *19*(3), 1867–1880. https://doi.org/10.5194/acp-19-1867-2019